








TECHNICAL ADVANCES

# Urine-derived lymphocytes as a non-invasive measure of the bladder tumor immune microenvironment

Yien Ning Sophia Wong<sup>1,2,3,4\*</sup>, Kroopa Joshi<sup>1,2,5,6\*</sup>, Prमित Khetrapal<sup>7,8</sup>, Mazlina Ismail<sup>5</sup>, James L. Reading<sup>1,2</sup>, Mariana Werner Sunderland<sup>1,2</sup>, Andrew Georgiou<sup>1,2</sup> , Andrew J.S. Furness<sup>1,2,6</sup> , Assma Ben Aissa<sup>1,2</sup>, Ehsan Ghorani<sup>1,2</sup>, Theres Oakes<sup>5</sup>, Imran Uddin<sup>5</sup>, Wei Shen Tan<sup>7,8</sup> , Andrew Feber<sup>8</sup> , Ursula McGovern<sup>4</sup>, Charles Swanton<sup>9</sup> , Alex Freeman<sup>10</sup>, Teresa Marafioti<sup>10</sup>, Timothy P. Briggs<sup>7</sup>, John D. Kelly<sup>7,8</sup>, Thomas Powles<sup>11</sup>, Karl S. Peggs<sup>1,2</sup>, Benjamin M. Chain<sup>5</sup> , Mark D. Linch<sup>3,4</sup>, and Sergio A. Quezada<sup>1,2</sup> 

**Despite the advances in cancer immunotherapy, only a fraction of patients with bladder cancer exhibit responses to checkpoint blockade, highlighting a need to better understand drug resistance and identify rational immunotherapy combinations. However, accessibility to the tumor prior and during therapy is a major limitation in understanding the immune tumor microenvironment (TME). Herein, we identified urine-derived lymphocytes (UDLs) as a readily accessible source of T cells in 32 patients with muscle invasive bladder cancer (MIBC). We observed that effector CD8<sup>+</sup> and CD4<sup>+</sup> cells and regulatory T cells within the urine accurately map the immune checkpoint landscape and T cell receptor repertoire of the TME. Finally, an increased UDL count, specifically high expression of PD-1 (PD-1<sup>hi</sup>) on CD8<sup>+</sup> at the time of cystectomy, was associated with a shorter recurrence-free survival. UDL analysis represents a dynamic liquid biopsy that is representative of the bladder immune TME that may be used to identify actionable immuno-oncology (IO) targets with potential prognostic value in MIBC.**

## Introduction

Immunotherapy trials targeting T cell checkpoint molecules and their ligands have demonstrated durable responses in patients with advanced bladder cancer. These results using monoclonal antibodies targeting programmed death-1 (PD-1; Nivolumab and Pembrolizumab) and programmed death-ligand 1 (PD-L1; Atezolizumab, Avelumab, and Durvalumab; Balar et al., 2017; Bellmunt et al., 2017; Powles et al., 2017, 2018; Sharma et al., 2017; Patel et al., 2018) have led to their approval by the US Food and Drug Administration as second line therapy or as first line therapy in patients ineligible for platinum-based chemotherapy.

Despite recent therapeutic advances and clinical successes of systemic immunotherapy in bladder cancer, ~75% of patients do not respond to treatment (Bellmunt et al., 2017; Sharma et al., 2017; Powles et al., 2018). To better understand drug resistance and inform the development of novel therapies and rational combinations of immunotherapeutic drugs, researchers have

focused on the characterization of the tumor immune microenvironment. To date, much attention has focused toward the evaluation of PD-L1 expression, mutational load and intra-tumoral T cell infiltration within tumor biopsy specimens taken before and/or during therapeutic intervention (Snyder et al., 2014; Rizvi et al., 2015; Van Allen et al., 2015; McGranahan et al., 2016; Mariathasan et al., 2018). However, in the vast majority of the patients, access to longitudinal tumor biopsies before and during the course of therapy remains a major limitation given the invasive nature of such procedures (Herbst et al., 2014; Tumei et al., 2014; Chen et al., 2016; Choueiri et al., 2016).

In patients with bladder cancer, the urine is a rich source of tumor-derived material that could potentially serve as a window to bladder tumor immune microenvironment. Several groups have investigated the use of urinary based biomarkers for the detection of bladder cancer, but their clinical use remains lim-

<sup>1</sup>Cancer Immunology Unit, University College London (UCL) Cancer Institute, London, England, UK; <sup>2</sup>Research Department of Haematology, UCL Cancer Institute, London, England, UK; <sup>3</sup>Department of Oncology, UCL Cancer Institute, London, England, UK; <sup>4</sup>Department of Oncology, University College London Hospital, London, England, UK; <sup>5</sup>Division of Infection and Immunity, University College London, London, England, UK; <sup>6</sup>Department of Medical Oncology, The Royal Marsden NHS Foundation Trust, London, England, UK; <sup>7</sup>Department of Urology, University College London Hospital at Westmoreland Street, London, England, UK; <sup>8</sup>Division of Surgical and Interventional Sciences, University College London, London, England, UK; <sup>9</sup>The Francis Crick Institute, London, England, UK; <sup>10</sup>Department of Cellular Pathology, University College London Hospital, London, England, UK; <sup>11</sup>Centre for Experimental Cancer Medicine, Barts Cancer Institute, Queen Mary University of London, London, England, UK.

\*Y.N.S. Wong and K. Joshi contributed equally to this paper; Correspondence to Sergio A. Quezada: [s.quezada@ucl.ac.uk](mailto:s.quezada@ucl.ac.uk); Mark D. Linch: [m.linch@ucl.ac.uk](mailto:m.linch@ucl.ac.uk).

© 2018 Wong et al. This article is distributed under the terms of an Attribution–Noncommercial–Share Alike–No Mirror Sites license for the first six months after the publication date (see <http://www.rupress.org/terms/>). After six months it is available under a Creative Commons License (Attribution–Noncommercial–Share Alike 4.0 International license, as described at <https://creativecommons.org/licenses/by-nc-sa/4.0/>).

ited by the sensitivity and specificity of the assays used (Chou et al., 2015). Urinary cell-free DNA has previously been demonstrated to reflect the bladder tumor genomic microenvironment (Birkenkamp-Demtröder et al., 2018), and urinary circulating tumor DNA (ctDNA; Togneri et al., 2016) has been associated with metastatic relapse in bladder cancer. Furthermore, increased numbers of urinary lymphocytes have been documented following intravesical Bacillus Calmette-Guerin immunotherapy in patients with non-muscle invasive bladder cancer (NMIBC; de Boer et al., 1991a; De Boer et al., 1991b; Pieraerts et al., 2012). However, in depth characterization of the expression of actionable immuno-oncology (IO) targets or their association with clinical outcome was not performed in any of these studies and patients with muscle invasive bladder cancer (MIBC) were not studied. Moreover, the extent to which urinary-derived markers reflect the tumor immune microenvironment remains unknown. In this study, we evaluated the phenotype of urinary-derived lymphocytes (UDLs) to determine their value in the identification of actionable IO targets expressed in the tumor microenvironment in patients with bladder cancer.

Here, we report for the first time that UDLs exhibit a T cell checkpoint phenotype and TCR repertoire reflective of the bladder tumor microenvironment and are associated with recurrence-free survival in patients with MIBC. Our data supports the further evaluation of UDLs as a non-invasive liquid biopsy that may be used to inform the activation status, checkpoint landscape, and TCR usage of tumor infiltrating lymphocytes (TILs) during the course of disease and throughout systemic therapy in patients with MIBC.

## Results

### Viable CD3<sup>+</sup> T lymphocytes are detected in the urine of a heterogeneous cohort of patients with MIBC

To determine whether lymphocytes could be detected in the urine of patients with MIBC, we collected precystectomy urine samples in 32 patients undergoing surgery with curative intent on the day of cystectomy. The most common histological subtype in the patients studied (27/32) was transitional cell carcinoma (TCC), and 5/32 patients were diagnosed with squamous cell carcinoma (SCC).

In our cohort, 13 patients were treatment naive (all with primary bladder tumors at surgery), and 19 patients received previous systemic (neoadjuvant chemotherapy or anti PD-L1) or intravesical therapy in the preceding 6 mo. Of the 19 patients who received prior therapy, 7 patients developed a complete pathological response that had been downstaged to pT0 disease (6/7) or carcinoma in situ (1/7). The remaining 12 patients had remaining pT2-T4 disease at cystectomy (no complete pathological response; Fig. 1 and Fig. S1). Tumor specimens were analyzed from a total of 25 patients with primary bladder tumors present at cystectomy (13 treatment naive and 12 patients following previous therapy). Based on previous studies (Daud et al., 2016), tissue, urine, or peripheral blood mononuclear cell (PBMC) samples containing <200 viable CD3<sup>+</sup> cells (as determined by flow cytometry) were considered nonevaluable for subsequent T cell subset and immune checkpoint analyses. In total, 24 urine, 25

tumor, 31 non-tumor (NT) bladder tissue, and 32 PBMC samples were analyzed in the study.

The median volume of urine collected from this cohort was 50 ml (range, 15–250 ml) with a median viable CD3<sup>+</sup> count per milliliter of 48.3 (range, 0.1–4,928.9). Irrespective of prior therapy, histology, complete pathological response, and stage, we were able to identify 200 or more viable CD3<sup>+</sup> UDLs in 20/25 (80%) of patients with primary bladder tumors present (at least pT2) and 4/7 (57.1%) patients who developed a complete pathological response (Fig. 1 and Fig. S1). CD3<sup>+</sup> UDLs were further divided into CD8<sup>+</sup>, CD4<sup>+</sup>FoxP3<sup>-</sup> (CD4<sup>eff</sup>), and CD4<sup>+</sup>FoxP3<sup>+</sup> (T reg) subsets as shown in Fig. 1, with matched TILs, NT lymphocytes, and PBMC as shown in Fig. S1. These T cell subsets were gated based upon CD3<sup>+</sup> within the lymphocyte gate (FSC-A by SSC-A), excluding doublets and nonviable cells. To exclude the possibility that UDL counts were associated with urinary infection, patients recruited to the study with a urine dipstick test positive for nitrites were excluded from the cohort. As a control, we also analyzed the urine of an age-matched cohort of six healthy volunteers being investigated for hematuria (Table S1). Importantly, there was an absence of lymphocytes within the urine of these healthy volunteers with no known bladder pathology.

### UDLs exhibit a similar checkpoint landscape to TILs independent of prior therapy

Having identified T lymphocytes in the urine of patients with MIBC, we sought to determine whether the immune checkpoint landscape of CD8<sup>+</sup>, CD4<sup>eff</sup>, and T reg in UDLs would faithfully represent that of lymphocytes found within bladder tumor microenvironment and NT, gated based upon viable CD3<sup>+</sup>. Due to their immediate clinical relevance, we focused our analysis on the expression of key coinhibitory and costimulatory immune checkpoints including PD-1, TIM-3, CTLA-4, ICOS, and 4-1BB.

Flow cytometric analysis revealed remarkable similarities in the distribution of checkpoints among effector CD8<sup>+</sup> and CD4<sup>+</sup> cells and T reg cells present in UDLs, tumor, and NT tissue that were significantly different to PBMC (Fig. S2 A). Significantly higher levels of PD-1 were found on effector CD4<sup>+</sup> and CD8<sup>+</sup> T cells within the urine, tumor, and NT compared with PBMCs. Moreover, increased ICOS and CTLA-4 expression on CD4<sup>eff</sup> and T reg cells in UDLs, TILs, and NT was detected, as compared with PBMC (Fig. 2 A and Fig. S2 A), consistent with previous studies (Liakou et al., 2008). Of relevance, the overall pattern of immune checkpoint distribution between UDLs, tumor, and NT tissue was consistent regardless of prior therapeutic intervention (Fig. 2 B and Fig. S2 A). The costimulatory receptor 4-1BB was partially up-regulated on UDL T reg cells compared with PBMCs, a trend that was also observed in TILs independent of prior therapy. Lastly, TIM-3 was up-regulated in both T reg and CD8<sup>+</sup> cells predominantly within TILs and UDLs (Fig. 2, A and B; and Fig. S2 A). We also observed high levels of TIM-3, ICOS, and CTLA-4, in addition to PD-1, on UDLs and TILs from patients with SCC (Fig. S2 C). Principal component analysis (PCA) was used as an unsupervised technique to further analyze the tumor and urine. The PCA values represent a summary of the frequencies of immune checkpoints for the T cell subsets studied in the

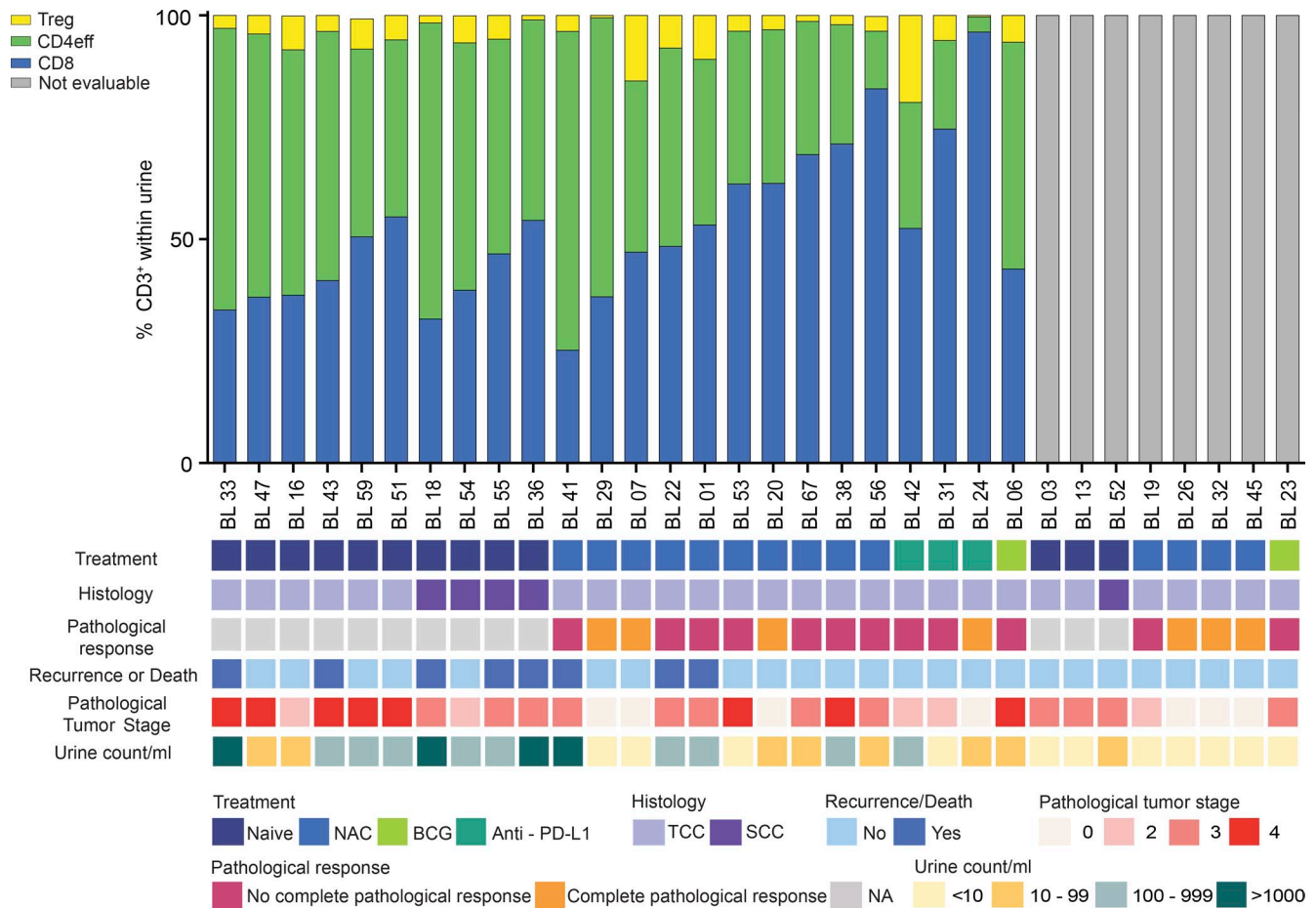


**Figure 1. Viable CD3<sup>+</sup> T lymphocytes are detected in the urine of a heterogeneous cohort of patients with MIBC.** The proportion of CD8<sup>+</sup>, CD4<sup>+</sup> FoxP3<sup>-</sup> (CD4eff), and CD4<sup>+</sup> FoxP3<sup>+</sup> (T reg) cells present within the viable CD3<sup>+</sup> gate in the urine is shown. Samples containing <200 viable CD3<sup>+</sup> on flow cytometry were deemed unevaluable for further T cell subset analysis and are highlighted in gray (not evaluable). Each patient’s prior treatment history, histological diagnosis, complete pathological response to therapy, clinical outcome (recurrence or death), pathological tumor stage, and urine count per milliliter is shown. No complete pathological response was defined as presence of pT2–T4 disease. A complete pathological response was defined as pT0 disease. BCG, Bacillus Calmette-Guerin; NA, not applicable; NAC, neoadjuvant chemotherapy; PD-L1, programmed death-ligand 1.

matched tumor and urine samples for each patient. These PCA values showed a positive correlation with a trend toward statistical significance (Spearman’s Rank correlation coefficient, 0.53;  $P = 0.057$ ; Fig. S2 B).

Having found key differences in the checkpoint distribution between TILs, UDLs, and NT compared with PBMCs, we compared the expression of multiple checkpoints on CD8<sup>+</sup> and CD4<sup>+</sup> effector T cells to interrogate the phenotypic overlap between TILs and UDLs, compared with NT tissue. Using all possible co-expression checkpoint phenotypes of CD8<sup>+</sup> and CD4eff, an unsupervised hierarchical clustering analysis of CD8<sup>+</sup> and CD4eff checkpoint expression showed that UDLs and TILs had a more similar co-expression checkpoint landscape compared with NT (Fig. 2 C and Fig. S3 A). To delineate the checkpoint phenotype most likely to account for the clustering of TILs and UDLs, we focused on the two checkpoint co-expression phenotypes with the largest delta in frequency between TILs and NT (Table S2). Within CD8<sup>+</sup> T cells, we found that the hierarchical clustering of UDLs and TILs was predominantly driven by PD-1/TIM-3, followed by PD-1/ICOS co-expression on CD8<sup>+</sup> T cells. In contrast, the similarity observed between effector CD4<sup>+</sup> T cells within TILs

and UDLs was largely accounted for by ICOS/CTLA-4, followed by CTLA-4/TIM-3 coexpression (Table S2).

In line with the above, the frequency of CD8<sup>+</sup> cells coexpressing PD-1/TIM-3 was significantly higher in UDLs and TILs as compared with NT tissue (Fig. 2 D). Importantly, no significant difference was observed in the frequency of CD8<sup>+</sup> coexpressing PD-1/TIM-3 between UDLs and TILs (Fig. 2 D), suggestive of chronic antigenic stimulation of CD8<sup>+</sup> cells found within the tumor and urine, compared with NT. Among the effector CD4<sup>+</sup> T cell compartment, the frequency of cells coexpressing ICOS and CTLA-4 was similar in UDLs and TILs (Fig. S3 B).

The data obtained from three patients selected as representative of the different histological subtypes and treatment histories in our cohort (BL 33, TCC treatment naive; BL 55, SCC treatment naive; BL 42, TCC neoadjuvant anti-PD-L1) was analyzed using the visualization software: Simplified Presentation of Incredibly Complex Evaluations (SPICE; Roederer et al., 2011). This different mode of analysis also showed a high degree of concordance in the coexpression phenotype of CD8<sup>+</sup> (Fig. 2 E) and CD4eff (Fig. S3 C) among UDLs and tumor with remarkably high levels of PD-1/TIM-3 coexpression on CD8<sup>+</sup>

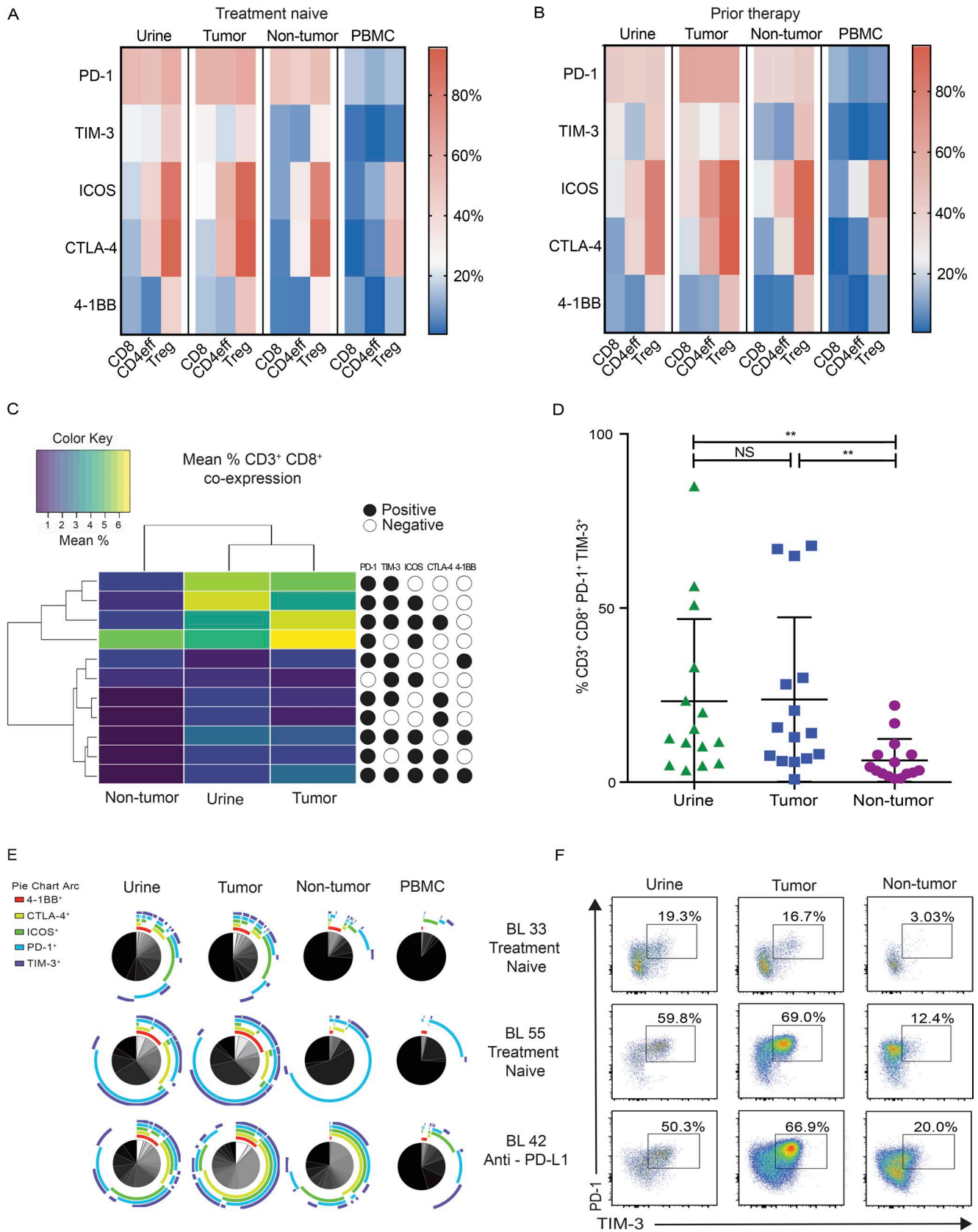


Figure 2. **UDLs exhibit a similar checkpoint landscape to tumor-infiltrating lymphocytes independent of prior therapy.** Single level expression and coexpression of B7 and TNFR superfamily coinhibitory and costimulatory molecules on T cell subsets were quantified by flow cytometry in matched urine, tumor, NT tissue, and PBMCs obtained from all patients. **(A and B)** Heat map depicts the mean percentage of CD8<sup>+</sup>, CD4<sup>eff</sup>, and T reg cells expressing individual immune checkpoint molecules in urine, tumor, NT, and PBMC samples obtained from treatment naive patients (*n* = 13; A), and patients that received prior systemic



(Fig. 2, D and F) and ICOS/CTLA-4 coexpression (on CD4eff (Fig. S3, B and D).

Collectively, the findings above are consistent with our hypothesis that the UDL population is largely derived from cells shed from the tumor into the urine and represent a window to the checkpoint landscape of lymphocytes within the tumor in patients with MIBC.

### The TCR repertoire of UDLs reflects the intra-tumoral repertoire

Since each TCR sequence is produced with very low probability (Murugan et al., 2012), two T cells expressing the same TCR sequence are likely to be part of the same clone. The TCR repertoire therefore provides a powerful way to probe how two T cell populations are related. We therefore sequenced the TCR repertoires of UDLs, tumor, NT tissue, and PBMCs in a subgroup of patients with matched RNA available. The total numbers of  $\alpha$  and  $\beta$  complementary determining region 3 (CDR3s) that were sequenced in each of the compartments are shown in the Table S3. A strong correlation was observed between the number of  $\alpha$  and  $\beta$  TCRs sequenced, reflecting the reproducibility of the sequencing method (Spearman's Rank correlation coefficient, 0.96;  $P < 0.0001$ ).

The TCR abundance distribution (i.e., the proportion of the repertoire which is made up of TCRs which occur only once, twice, three times, etc.) of the four populations combined from all the patients is shown for  $\beta$  TCRs (Fig. 3 A) and for  $\alpha$  TCRs (Fig. S4 A). The clonal structure of the TCR repertoire was similar across tumor, urine, NT tissue, and PBMC samples, therefore any differences observed in the TCR landscape of these compartments was unlikely due to differences in the distribution of the repertoire of T cells.

Having noted a similar TCR distribution across all of the compartments studied, we next examined the relationship between the repertoires at the level of the individual CDR3 sequences. For each individual patient, unsupervised hierarchical clustering of CDR3 frequencies reproducibly clustered the urine TCR sequences with the tumor TCR sequences for  $\beta$  (Fig. 3 B) and  $\alpha$  (Fig. S4 B). To confirm the statistical significance of this relationship, we modeled the urine as a subsample of one of the other populations. We repeatedly sampled from each repertoire and measured the Jaccard index and repertoire similarity of each sample with an equal sized sample from the urine repertoire (see Materials and methods for details). This bootstrap approach allowed us to compare the repertoire similarity between the urine and other samples quantitatively. As shown in Fig. 3

(C and D), for  $\beta$  TCRs, the similarity of urine to the tumor was much greater than to either NT tissue or blood ( $P < 0.0001$ ), whether using the Jaccard index, which measures the number of shared sequences without regard to abundance, or the similarity metric, which takes into account the abundance of the shared CDR3s. This pattern was also observed within the  $\alpha$  TCR repertoire (Fig. S4, C and D).

Expanded T cell clones within the tumor may represent an important source for the cellular immunotherapy of cancer. We therefore examined whether TCRs found at high abundance within the tumor could also be found within urine, since urine would potentially provide an easier source of such cells for adoptive therapy protocols. Several of the 10 most abundant TCRs in tumor were indeed found within urine. In contrast, few of the expanded  $\alpha$  and  $\beta$  CDR3 sequences in the urine were found among the 10 most expanded CDR3 sequences in NT tissue and PBMC samples (Fig. 3 E and Fig. S4 E).

Together, these data demonstrate that the urine contains a population of lymphocytes that closely reflect the tumor infiltrating TCR repertoire and are suggestive of similar antigenic specificities of UDLs and TILs.

### Increased urinary CD3<sup>+</sup>CD8<sup>+</sup>PD-1<sup>hi</sup> lymphocytes are associated with a worse clinical outcome in patients with MIBC

Given that the T cell checkpoint phenotype and TCR repertoire underscored the role of UDLs as a surrogate for the TIL phenotype and TCR repertoire and that TILs have previously been associated with survival in various solid tumors (Gooden et al., 2011), we sought to determine whether the presence of T cells in the urine was associated with tumor stage, response, and/or recurrence-free survival in patients with MIBC. The 32 patients were followed up for a median time of 8 mo.

First, we assessed whether the UDL count, taken on the day of cystectomy (number of events recorded within viable CD3<sup>+</sup> gate on the flow cytometer) correlated with pathological tumor stage and treatment response as a low pathological stage and response to neoadjuvant therapy are associated with improved recurrence-free survival (Grossman et al., 2003). We used a standardized measure of UDL count (per milliliter of urine) given the variation of urine volumes collected within the patient cohort. Although a similar UDL concentration was found for patients with T0, T2, or T3 disease, a significantly higher UDL concentration was found in patients with T4 tumors compared with T0 tumors (median 150.6 vs. 5.45 UDL count/ml;  $P = 0.009$ ), suggesting that locally advanced tumors may be more likely to generate UDLs (Fig. 4 A). We also observed that those patients that

therapy ( $n = 19$ ; B). (C) Displayed is an unsupervised clustering heat map of the mean frequencies of CD8<sup>+</sup> cells demonstrating each of the coexpression immune checkpoint phenotypes in found tumor, urine, and NT tissue. Each row within the heat map represents a different immune checkpoint coexpression phenotype. Key represents the markers that define each of the coexpression phenotypes: presence of marker (black circles) or absence of marker (white circles). Only CD8<sup>+</sup> coexpression phenotypes found at a frequency of  $\geq 1\%$  (mean across all patients) in any of tumor, urine, or NT are shown. (D) Graph depicts the frequency of CD8<sup>+</sup> T cells that coexpress PD-1 and TIM-3 in tumor, urine, and NT samples. P values were calculated using paired t test. Bars represent mean values with SD. \*,  $P < 0.05$ ; \*\*,  $P < 0.005$ ; NS, not significant. (E) SPICE analysis of all CD8<sup>+</sup> T cells displaying the coexpression of checkpoint molecules in urine, tumor, NT, and PBMC in a representative group of patients (BL 33, TCC treatment naive; BL 55, SCC treatment naive; BL 42, TCC neoadjuvant immunotherapy). Pie charts depict qualitative distribution of checkpoint expressions on CD8<sup>+</sup> T cells. Arcs show checkpoint makeup and overlap within pie slice. (F) Coexpression pattern of PD-1/TIM-3 on CD8<sup>+</sup> on urine, tumor, and NT. Dot plots display the phenotype of CD8<sup>+</sup> lymphocytes from matched samples from the same representative patients in E (BL 33, BL 55, and BL 42). The percentage of cells expressing each combination of checkpoint molecules is shown.

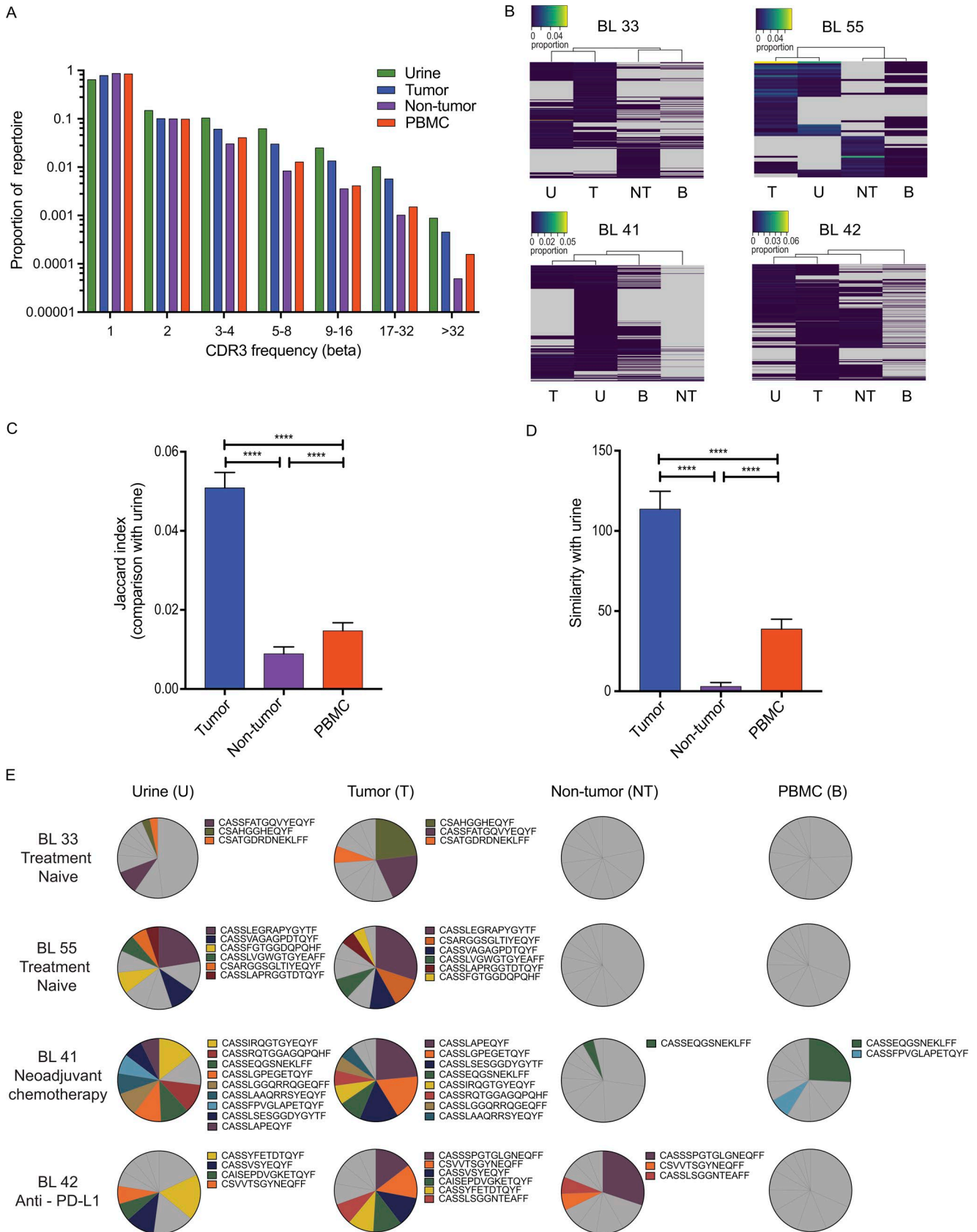


**Figure 3. The TCR repertoire of UDLs reflects the intra-tumoral repertoire. (A)** The distribution of  $\beta$  chain TCRs in the urine is similar to tumor, NT tissue, and PBMCs. The proportion of TCRs found with different abundances (x axis) in urine, tumor, NT tissue, and PBMCs is shown. **(B)** Hierarchical clustering of CDR3s demonstrates similarity in the TCR repertoire of urine and tumor. CDR3s were filtered based on abundance (present at least eight times) and detected in at least one of urine, tumor, or NT tissue. Color key represents the proportion of each CDR3 within the whole repertoire. T, tumor; U, urine; B, PBMC. **(C)** The overlap,

achieved a complete pathological response to systemic therapy had a significantly lower UDL count on the day of cystectomy as compared with patients that were treatment naive (median 5.45 vs. 194.1 UDL count per/ml;  $P = 0.03$ ; Fig. 4 B). However, there was no statistically significant difference in the UDL count among patients that had primary tumors present at surgery (treatment naive versus nonresponding patients). In addition, no significant difference in UDL count was observed between patients that achieved a complete pathological response and those that did not. We next evaluated whether UDL count could be associated with disease recurrence. We found that disease recurrence was significantly associated with a higher UDL concentration detected at the time of cystectomy (1,003 vs. 17.82 UDL count/ml,  $P < 0.0001$ ; Fig. 4 C).

When dividing patients into two groups based on the median UDL count, we observed that patients with a low UDL count (below the median) did not develop recurrence of their disease (Fig. 4 D), in contrast to patients with a high UDL concentration that had a poorer recurrence-free survival (UDL count above the median;  $P = 0.0004$ ). Next, when considering UDL count as a continuous variable and performing a natural log transformation (Fig. S5 A), the unadjusted hazard ratio (HR) was calculated as 1.80 (95% confidence interval [CI], 1.22–2.63;  $P = 0.003$ ).

Given the potential confounding effect of tumor stage and treatment response on the UDL count, we performed statistical adjustment for these variables using a Cox regression model (Fig. S5 A). Notably the association between higher UDL count/ml and a poorer recurrence-free survival remained statistically significant when adjusted for pathological tumor stage (adjusted HR, 1.49; 95% CI, 1.02–2.17;  $P = 0.04$ ), or treatment response with an adjusted HR of 1.61 (95% CI, 1.06 – 2.46;  $P = 0.026$ ). The multivariate analysis when stratified for both tumor stage and response was not statistically significant, with an adjusted HR of 1.43 (95% CI, 0.92–2.21,  $P = 0.108$ ).

Having observed that patients with an increased urinary CD3<sup>+</sup> count were more likely to experience disease relapse, we next assessed whether there were any checkpoint phenotypes that may account for this result. We did not observe any significant differences in survival when considering urinary CD3<sup>+</sup>PD-1<sup>+</sup> or CD8<sup>+</sup>PD-1<sup>+</sup>TIM-3<sup>+</sup> cells. Previous work has shown that CD8<sup>+</sup> TILs with the highest expression of PD-1 is associated with tumor reactivity, reflective of chronic antigenic stimulation resulting in a dysfunctional and exhaustive state (Blackburn et al., 2008; Paley et al., 2012; Thommen et al., 2015, 2018; Reading et al., 2018). In line with previous work, (Thommen et al., 2018) we classified CD8<sup>+</sup>PD-1<sup>+</sup> T cells into high and low categories; cells considered to be PD-1<sup>hi</sup> were those with expression levels of PD-1 expression greater than that observed in matched PBMC samples (Fig. S5 B). We next considered whether an increased frequency of levels of PD-1<sup>hi</sup> CD8<sup>+</sup> UDLs was related to survival.

Interestingly, we observed that the frequency of CD8<sup>+</sup>PD-1<sup>hi</sup> cells was significantly higher in UDLs ( $P = 0.01$ ) and TILs ( $P = 0.0004$ ) as compared with NT tissue (Fig. 4 E). Importantly, no significant difference was observed in the frequency of CD8<sup>+</sup>PD-1<sup>hi</sup> cells between UDLs and TILs (Fig. 4 E), suggestive of chronic antigenic stimulation of these cells. The natural log UDL CD3 count/ml significantly correlated with CD8<sup>+</sup>PD-1<sup>hi</sup> expression in both UDLs (Spearman's Rank correlation coefficient, 0.62;  $P = 0.0012$ ; Fig. 4 F) and TILs (Spearman's Rank correlation coefficient, 0.68;  $P = 0.0002$ ; Fig. S5 C). Finally, we demonstrated that patients with increased levels of CD8<sup>+</sup>PD-1<sup>hi</sup> cells (above the median) were more likely to develop recurrence of their disease compared with those with low levels of CD8<sup>+</sup>PD-1<sup>hi</sup> (below the median), with a highly significant  $P$  value of 0.0009, with an unadjusted HR of 4.3 (95% CI, 1.02–18.23;  $P = 0.048$ ).

Collectively, these data highlight the potential prognostic role of the UDL count and CD8<sup>+</sup> phenotype in patients with MIBC that requires validation in a prospective study.

## Discussion

Our results demonstrate for the first time that urine-derived lymphocytes in patients with MIBC exhibit a T cell checkpoint phenotype and TCR repertoire that overlaps with lymphocytes infiltrating the bladder tumor microenvironment. Remarkably, this similarity was observed in a heterogeneous cohort of 32 patients undergoing cystectomy that included patients with different stages of disease, treatment histories, and histological subtypes. Furthermore, we demonstrated that patients with a high urinary lymphocyte count were more likely to relapse of bladder cancer, reflecting the potential prognostic value of UDL analysis.

Given the similarity in the coexpression T cell checkpoint landscape and TCR repertoire between UDLs and TILs and the absence of UDLs in the urine of healthy individuals (Table S1), it is plausible that UDLs are derived from the tumor tissue itself, although the mechanisms by which lymphocytes enter the urine remain elusive. Factors that may regulate release of TILs into the urine include the extent of tumor invasion, necrosis, or microvessel density, resulting in leakage and exfoliation of tumor cells and infiltrating lymphocytes into the urine, all of which would be worthy of future study.

Current clinical studies in bladder cancer typically include the collection of peripheral blood samples in an attempt to gain insight into the evolving bladder tumor microenvironment. Strikingly, our data demonstrate minimal phenotypic and repertoire overlap between PBMC and TILs and instead suggest that UDLs better recapitulate the bladder T cell and immune checkpoint landscape that may be relevant for future clinical studies.

The overlap between TILs and UDLs was well exemplified by similarly high levels of PD-1 and TIM-3 CD8<sup>+</sup> coexpression in

quantified by the Jaccard index, between the set of CDR3s found in urine and in each of the other compartments is shown. The results show the mean plus SD. The significance was measured by one-way ANOVA. (D) Similarity index (measured as the dot product of the abundances) between samples of the urine TCR repertoire and the repertoire of each other compartment. The results show the mean plus SD. The significance was measured by one-way ANOVA. (E) The most expanded CDR3s detected in the tumor are also expanded within the urine. Pie charts represent the 10 most abundant  $\beta$ CDR3s ranked in descending order in the urine, tumor, NT, and PBMCs. CDR3s among the top 10 CDR3s present in at least two of tumor, urine, tumor, NT tissue, and PBMCs are highlighted in color. Gray represents CDR3s that are not shared. \*\*\*\*,  $P < 0.0001$  for C and D.

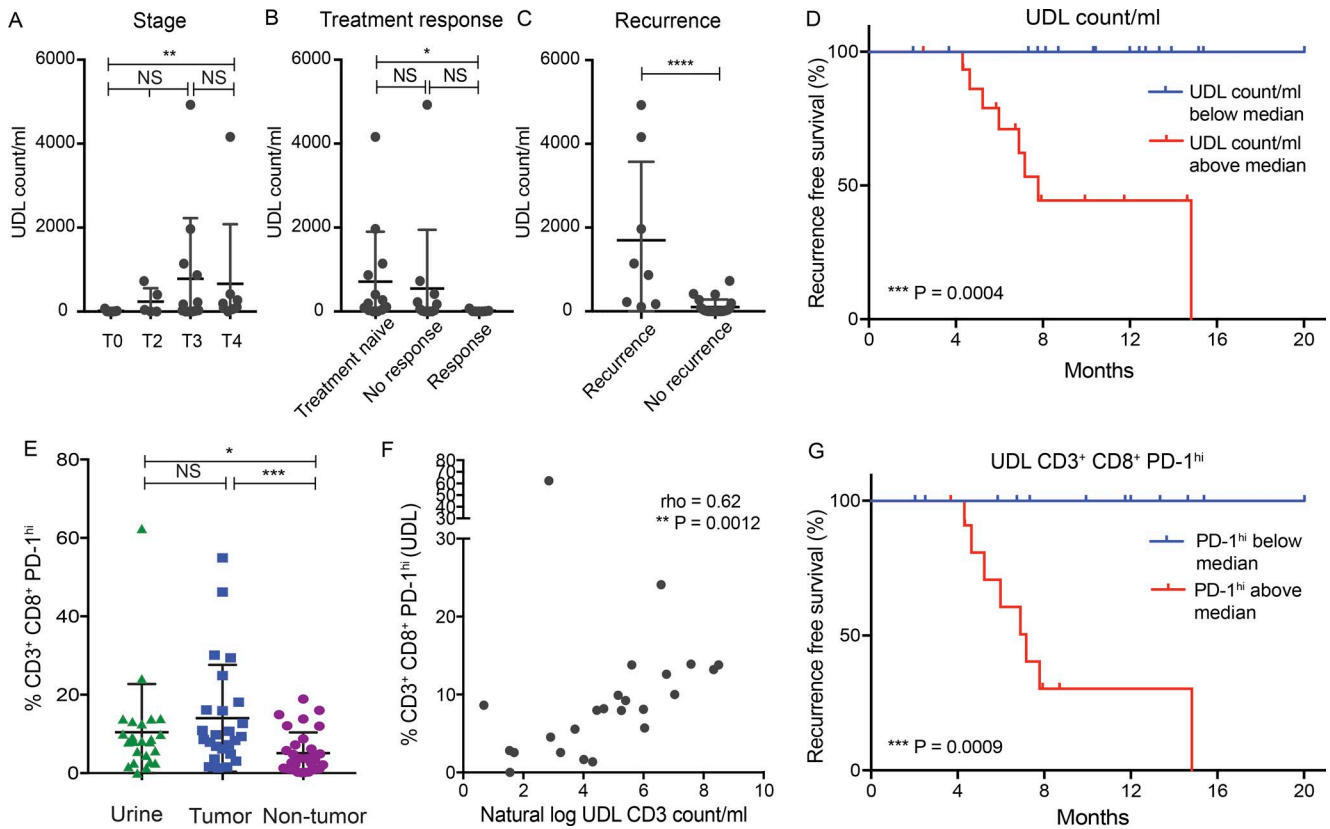


**Figure 4. Increased urinary CD3<sup>+</sup>CD8<sup>+</sup>PD-1<sup>hi</sup> lymphocytes are associated with a worse clinical outcome in patients with MIBC.** Displayed is the association of urinary lymphocyte count with clinical outcome. **(A and B)** UDL count/ml and relationship with pathological tumor stage (A) and response to treatment (B) is shown. **(C)** The association of disease recurrence and UDL count is shown. Mann-Whitney *U* test used for statistical analysis. Error bars represent mean values with SD. **(D)** Recurrence-free survival (%) over a median follow up of 8 mo is shown according to whether patients were found to have a high UDL count (above the median) or a low UDL count (below the median). **(E)** Graph depicts the frequency of CD8<sup>+</sup>PD-1<sup>hi</sup> T cells in tumor, urine, and NT tissue samples. Mann-Whitney *U* test used for statistical analysis. Error bars represent mean values with SD. **(F)** Displayed is a Spearman rank correlation of the frequency of CD3<sup>+</sup>CD8<sup>+</sup>PD-1<sup>hi</sup> in UDL (%) and the natural log CD3 count/ml in urine samples. Spearman rank correlation coefficient and P values shown. **(G)** Recurrence-free survival (%) over a median follow up of 8 mo is shown according to whether patients had a high frequency of PD-1<sup>hi</sup> (above the median) or a low frequency of PD-1<sup>hi</sup> (below the median). \*, *P* < 0.05; \*\*, *P* < 0.005; \*\*\*, *P* < 0.0005; \*\*\*\*, *P* < 0.0001; NS, not significant for A–C and E.

both compartments: a phenotype associated with chronic antigenic stimulation and impaired T cell function (Sakuishi et al., 2010; Gros et al., 2014). We also observed similar levels of ICOS and CTLA-4 coexpression on CD4<sup>eff</sup> within TILs and UDLs. A similar expression pattern has been previously documented in bladder cancer CD4<sup>+</sup> TILs following anti-CTLA-4 therapy (Liakou et al., 2008). The phenotypic and repertoire concordances between TILs and UDLs across treated and untreated patients support the use of UDLs in the longitudinal evaluation of the bladder tumor immune microenvironment, for example in the context of immunotherapeutic clinical trials.

Given the array of checkpoint molecules expressed on the surface of lymphocytes within the urine, UDL analysis may also be used to explore the checkpoint landscape throughout therapy, with the potential to inform subsequent actionable IO targets in patients with MIBC. Given the high percentage of TIM-3, CTLA-4, and ICOS coexpressed with PD-1 on effector T cell subsets within the tumor microenvironment, further investigation exploring the therapeutic targeting of these molecules, either alone or in conjunction with PD-1/PD-L1 blockade, is warranted. A high level of TIM-3, ICOS, and CTLA-4, in addition to PD-1, was ob-

served on UDLs and TILs from patients with SCC. Of relevance, this is a histological subtype largely excluded from clinical trials of checkpoint blockade, with limited treatment options in the clinical setting. Our findings suggest that patients with SCC may benefit from immunotherapy directed against these targets and may warrant inclusion in future clinical trials.

In addition to checkpoint molecules, the use of TCR repertoire analysis of UDLs may be used as a tool to track T cell dynamics throughout immunotherapy, providing insight into the specificity of immune response. Whether RNA from UDLs could also be used to characterize and unveil changes in the transcriptional program of tumor-reactive T cells through therapy remains to be determined. Moreover, given the potential tumor reactivity of UDLs, they may provide a convenient and easily accessible source of cells for *in vitro* expansion and subsequent adoptive cellular immunotherapy for patients with MIBC, although this needs to be explored further.

The demonstration that the UDL phenotype and repertoire overlaps with tumor lymphocyte populations, and that the number of UDLs is related to disease outcome suggests that UDL analysis may complement the use of urinary ctDNA in pa-



tients with bladder cancer in combination, providing insight into both the immune and genetic landscape within the tumor microenvironment.

Our findings also demonstrated that patients were 1.8 times more likely to relapse of bladder cancer for every log unit increase in UDL count. Moreover, we found that an increased UDL count was associated with pathological tumor stage and response to systemic therapy, highlighting the intricate relationship between UDL count, tumor stage, and treatment response. While increased intra-tumoral T cell infiltration has previously been associated with improved clinical outcome in a variety of tumor types including MIBC (Sharma et al., 2007), our data suggest that the presence of UDLs are associated with a worse clinical outcome. Importantly, UDL count and TIL count are two separate entities, and an increased TIL count may be reflective of an ongoing anti-tumoral immune response, as previously described, thus associated with a favorable clinical outcome (Gooden et al., 2011).

The biological significance of an increased UDL count was subsequently explored to gain a better understanding of the possible underlying mechanism(s) that may explain the observed relationship between increased UDL count and poorer clinical outcomes. Given that PD-1 expression has previously shown to identify tumor reactive T cells (Inozume et al., 2010; Gros et al., 2014; McGranahan et al., 2016), and T cells with the highest level of PD-1 expression are associated with distinct transcriptomic, phenotypic, and functional properties (Thommen et al., 2015, 2018; Reading et al., 2018; Zappasodi et al., 2018), we next assessed the PD-1 expression levels of UDLs and correlated this with clinical outcome. We observed a similar frequency of CD8<sup>+</sup>PD-1<sup>hi</sup> cells in urine and tumor samples, which was significantly higher than NT tissue. Additionally, a significant positive correlation was observed between UDL count/ml and the frequency of CD8<sup>+</sup>PD-1<sup>hi</sup> UDLs and TILs. The mechanism underlying this observation currently remains unclear, but may be reflective of (1) tumor inflammation, (2) expansion and/or differentiation of CD8<sup>+</sup>PD1<sup>hi</sup> cells, in response to chronic tumor antigen exposure, and (3) loss of basement membrane integrity during antigen specific T cells responses in the bladder.

Importantly, we found that patients with increased frequency of CD8<sup>+</sup>PD1<sup>hi</sup> UDLs were more likely to experience disease relapse, highlighting the potential clinical relevance of CD8<sup>+</sup>PD1<sup>hi</sup> UDLs that requires further prospective validation. Moreover, increased PD-1 expression consistent with chronic antigenic exposure and T cell dysfunction has previously been correlated with worse disease-free survival in head and neck cancer (Kansy et al., 2017). While it is plausible that CD8<sup>+</sup>PD-1<sup>hi</sup> UDLs may point toward tumor reactivity, it is not possible to fully conclude this. Accordingly, further phenotypic and functional studies, including bulk RNA or single cell RNA sequencing aimed at evaluating the antigenic specificity and biological mechanisms leading to UDL generation warrant further investigation.

We recognize that our findings are based on a relatively small sample size of a heterogeneous cohort of patients in terms of histological subtype, treatment histories, and treatment response. However, despite the marked heterogeneity, the flow phenotype and TCR repertoire remain similar between urine and tumor, suggesting that urinary lymphocytes are dynamic and may be able

to recapitulate the tumor microenvironment at that time point. Further prospective studies in a larger cohort of patients, considering the above, are required to corroborate our preliminary findings and validate the hypothesis that UDL count and phenotype is prognostic in MIBC. Importantly, UDL analysis is most relevant in patients who have not undergone cystectomy. It is estimated that ~60% of patients with metastatic bladder cancer present with de novo metastatic disease with the primary bladder cancer in situ (Pal et al., 2015). In addition, approximately a quarter of patients with metastatic bladder cancer will have received bladder sparing primary therapy such as radiotherapy, with a proportion likely to have tumor relapse within the bladder. Thus, UDL analysis is not only likely to have utility in the assessment of patients with muscle invasive localized disease, but could be important for the longitudinal evaluation of patients with metastatic bladder cancer with their primary bladder cancer in situ undergoing systemics therapy. Indeed, for this latter group, our preliminary data show the presence of UDLs and indicated dynamic immune checkpoint phenotype changes throughout therapy (unpublished data). This is work that is ongoing and an area of future study. Lastly, our current study is very much T cell focused, and we plan to explore the urinary myeloid compartment in subsequent studies.

In conclusion, we have identified UDLs as a readily accessible source of T cells from patients with MIBC that accurately map the immune landscape and repertoire of lymphocytes within the tumor microenvironment within a heterogeneous cohort of patients. These findings warrant a trial in a larger independent cohort of patients to firmly validate the use of UDL analysis as a novel, clinically useful liquid biopsy with potential prognostic implications.

## Materials and methods

### Study design

Matched bladder tumor, NT tissue urothelium, urine, and PBMCs were collected from 32 patients undergoing radical cystectomy. The patient cohort comprised of those initially diagnosed with MIBC. The cohort included patients that were either treatment naive ( $n = 13$ ) or those that had received prior therapy (chemotherapy, immunotherapy, or Bacillus Calmette-Guerin) during the 6 mo preceding cystectomy ( $n = 19$ ).

### Isolation of lymphocytes from peripheral blood and urine

On the day of radical cystectomy, fresh urine and blood samples were obtained before the start of surgery. Peripheral blood was collected into 10-ml EDTA tubes. Urine was collected in the morning of cystectomy into a universal container. All urine samples were tested by dipstick for the presence of infection. Any sample that tested positive for nitrites was excluded from further analyses. PBMC and UDLs were isolated through density-gradient centrifugation using Ficoll-Paque PLUS (GE Healthcare). Live cells were stained fresh following isolation. Excess sample not used for staining was frozen at  $-80^{\circ}\text{C}$  and stored in liquid nitrogen.

### Isolation of lymphocytes from tumor and NT tissue samples

Following radical cystectomy, the bladder specimen was dissected, and NT tissue was sampled from the contralateral side

to the tumor as identified macroscopically. All tissue samples were placed into conical tubes containing plain RPMI culture medium (Sigma) and transferred locally on the day of collection for processing. Tumor samples were micro dissected manually and digested with Collagenase (2.5 mg/ml; Gibco) and DNase I (0.2 mg/ml; Roche) at 37°C for 1 h, homogenized using gentle-MACS (Miltenyi Biotech), and filtered through a 0.7- $\mu$ m cell mesh. Leukocytes were enriched by gradient centrifugation with Ficoll-paque (GE Healthcare). Once isolated, single cell suspensions of lymphocytes were stained fresh on the day of processing. Excess sample not used for staining was frozen at -80°C and stored in liquid nitrogen. All tissue samples from cystectomy were verified using immunohistochemistry by a consultant histopathologist specializing in uro-oncology.

### Flow cytometry

Acquisition was performed with a BD LSR II Fortessa (BD Biosciences). The following antibodies and fluorescent labels were used in the flow cytometry experiments: from Biolegend, PD-1-Q605 (EH12.2H7), CD25-BV711 (BC96), CD3-BV785 (OKT3), CTLA-4-APC (L3D10), ICOS-APC (C398.4A), and 4-1BB-PE (4B4-1); from BD Biosciences, Granzyme B-V450 (GB11), CD8-V510 (SK1), and TIM-3-Q650 (7D3); from eBioscience, FoxP3-PE (PCH101), CD4-AF700 (OKT4), and fixable viability dye-e780. Intranuclear staining of FoxP3 and Ki67 was performed using the FoxP3 Transcription Factor Staining Buffer Set (eBioscience).

### TCR sequencing

The  $\alpha$  and  $\beta$  chains of the TCR repertoire were sequenced using a method which starts with total RNA isolated from unfractionated tissue/cells and introduces unique molecular identifiers attached to individual cDNA molecules to provide a quantitative and reproducible method of library preparation. RNA was extracted from tissue or PBMC samples using standard silica membrane columns (AllPrep DNA/RNA Mini kit or RNeasy Micro or Mini kits; Qiagen). Full details for both the experimental library preparation and the subsequent computational analysis using Decombinator is published in [Oakes et al. \(2017\)](#). For each sample, the output provides a list of CDR3 sequences and the number of times each CDR3 is observed.

The Jaccard index between two repertoires is calculated as the intersection between two sets of TCRs (i.e., the number of shared CDR3 sequences) divided by the union (the sum of the number of unique sequences in both sets). The similarity between two samples was measured using a standard similarity metric, calculated as the dot product between the vector of CDR3 frequencies in each sample. In [Fig. 3 \(C and D\)](#), we subsampled the combined repertoires from each compartment. Each sample contained 1,000 unique CDR3s. Each sample from tumor, NT tissue and blood was compared with an equal sized sample from the urine. The sampling was repeated 100 times, and the figure shows the average and SD. Statistical analysis was performed using a one-way ANOVA.

### Flow cytometry statistical analysis

Flow cytometry data analysis was performed in FlowJo version 10.0.8 (Tree Star Inc.). Statistical analyses were performed in

Prism 6 (GraphPad Software, Inc.); P values were calculated using Kruskal-Wallis analysis of variance and Dunn's post-hoc test with error bars represent mean values with SEM, unless otherwise indicated in the figure legends (NS,  $P > 0.05$ ; \*,  $P \leq 0.05$ ; \*\*,  $P \leq 0.01$ ; \*\*\*,  $P \leq 0.001$ ; \*\*\*\*,  $P \leq 0.0001$ ).  $<200$  viable CD3<sup>+</sup> cells were defined as inadequate number of cells for analysis. Analysis of Kaplan-Meier survival curves was performed with use of the log-rank test.

### Human study oversight

Collection of human tissue for this study was agreed by the institutional review board as part of the University College London/University College London Hospital BioBank for Health and Human Disease (REC 15/YH/0311) study. All patients (or their legal representatives) provided written informed consent before enrolment.

### Online supplemental material

Fig. S1 shows the proportion of T cell subsets within CD3<sup>+</sup> T lymphocytes in matched tumor, NT tissue, and PBMCs. Fig. S2 supports the findings in [Fig. 2](#), showing the statistical evaluation of the immune checkpoint molecule expression on the T cell subsets, including SCC. In [Fig. S3](#), effector CD4<sup>+</sup> T cells also exhibit a similar coexpression checkpoint phenotype in UDLs and TILs. [Fig. S4](#) demonstrates the corresponding  $\alpha$  TCR repertoire of UDLs, which reflects the intra-tumoral repertoire. [Fig. S5](#) complements [Fig. 4](#), showing that increased urinary CD3<sup>+</sup>CD8<sup>+</sup>PD-1<sup>hi</sup> lymphocytes are associated with a worse clinical outcome in patients with MIBC. The UDL counts in age-matched patients with no known bladder pathology are shown in Table S1. Table S2 demonstrates the delta frequency difference between tumor and NT tissue checkpoint coexpression phenotypes within the effector T cells in descending order. The largest delta frequencies were used for [Fig. 2 \(D and F\)](#) and [Fig S3 \(B and D\)](#). Finally, Table S3 shows the total numbers of  $\alpha$  and  $\beta$  CDR3s sequenced.

### Acknowledgments

We thank Andre Lopes from the University College London (UCL) Cancer Trials Centre for his valuable statistical advice and Ashwin Sridhar, Benjamin Lamb, Mohammed Abozaid, Darren Goh, Melanie Tan, and Hilary Baker from the Department of Urology at UCL for providing clinical specimens. We thank all the patients that participated in this study.

S.A. Quezada is a Cancer Research U.K. (CRUK) Senior Fellow (C36463/A22246) and is funded by a Cancer Research Institute Investigator Award and a CRUK Biotherapeutic Program Grant (C36463/A20764). M.D. Lynch, B.M. Chain, and C. Swanton receive funding from the National Institute for Health Research (NIHR), UCL Hospitals Biomedical Research Centre, and M.D. Lynch is supported by the CRUK UCL Experimental Cancer Medicine Centre. K.S. Peggs receives funding from the NIHR Blood & Transplant Research Units (BTRU) for Stem Cells and Immunotherapies (167097), of which he is the Scientific Director. This work was undertaken at UCL/UCL Hospitals with support from the CRUK-UCL Centre (Y.N.S. Wong; grant no. C416/A18088), the Cancer Immunotherapy Accelerator Award (CITA-CRUK;

C33499/A20265), the Sam Keen Foundation and The Royal Marsden Hospital NHS Foundation Trust NIHR Biomedical Research Centre (K. Joshi), Bloodwise (formerly Leukaemia and Lymphoma Research; 08022/P4664), the NIHR UCL Hospitals Biomedical Research Centre (B.M. Chain), and a CRUK Project Grant (B.M. Chain). The funders had no role in study design, data collection and analysis, decision to publish, or preparation of the article. This work was supported by the Francis Crick Institute, which receives its core funding from Cancer Research UK (FC001169), the UK Medical Research Council (FC001169), and the Wellcome Trust (FC001169).

T. Powles receives research funding and honoraria from Roche, AstraZeneca, and Merck. All the other authors have no conflict of interest to disclose.

Author contributions: Y.N.S. Wong, K. Joshi, M.D. Lynch, and S.A. Quezada conceived the project, designed the experiments, analyzed the data, and wrote the manuscript. Y.N.S. Wong and P. Khetrpal recruited study participants; Y.N.S. Wong and K. Joshi performed the experiments. J.L. Reading, M.W. Sunderland, A. Georgiou, A.J.S. Furness, A.B. Aissa, T. Oakes, and I. Uddin contributed experimentally. M. Ismail and W.S. Tan contributed to data analysis. W.S. Tan, E. Ghorani, B.M. Chain, C. Swanton, T. Marafioti, and K.S. Peggs contributed scientifically. A. Feber, A. Freeman, U. McGovern, T.P. Briggs, J.D. Kelly, and T. Powles coordinated clinical trials and provided patient samples. All authors reviewed and approved the final manuscript.

Submitted: 29 May 2018

Revised: 3 August 2018

Accepted: 5 September 2018

## References

Balar, A.V., D. Castellano, P.H. O'Donnell, P. Grivas, J. Vuky, T. Powles, E.R. Plimack, N.M. Hahn, R. de Wit, L. Pang, et al. 2017. First-line pembrolizumab in cisplatin-ineligible patients with locally advanced and unresectable or metastatic urothelial cancer (KEYNOTE-052): a multicentre, single-arm, phase 2 study. *Lancet Oncol.* 18:1483–1492. [https://doi.org/10.1016/S1470-2045\(17\)30616-2](https://doi.org/10.1016/S1470-2045(17)30616-2)

Bellmunt, J., R. de Wit, D.J. Vaughn, Y. Fradet, J.-L. Lee, L. Fong, N.J. Vogelzang, M.A. Climent, D.P. Petrylak, T.K. Choueiri, et al. KEYNOTE-045 Investigators. 2017. Pembrolizumab as Second-Line Therapy for Advanced Urothelial Carcinoma. *N. Engl. J. Med.* 376:1015–1026. <https://doi.org/10.1056/NEJMoa1613683>

Birkenkamp-Demtröder, K., E. Christensen, I. Nordentoft, M. Knudsen, A. Taber, S. Hoyer, P. Lamy, M. Agerbaek, J.B. Jensen, and L. Dyrskjot. 2018. Monitoring Treatment Response and Metastatic Relapse in Advanced Bladder Cancer by Liquid Biopsy Analysis. *Eur. Urol.* 73:535–540. <https://doi.org/10.1016/j.eururo.2017.09.011>

Blackburn, S.D., H. Shin, G.J. Freeman, and E.J. Wherry. 2008. Selective expansion of a subset of exhausted CD8 T cells by alphaPD-L1 blockade. *Proc. Natl. Acad. Sci. USA.* 105:15016–15021. <https://doi.org/10.1073/pnas.0801497105>

Chen, P.L., W. Roh, A. Reuben, Z.A. Cooper, C.N. Spencer, P.A. Prieto, J.P. Miller, R.L. Bassett, V. Gopalakrishnan, K. Wani, et al. 2016. Analysis of Immune Signatures in Longitudinal Tumor Samples Yields Insight into Biomarkers of Response and Mechanisms of Resistance to Immune Checkpoint Blockade. *Cancer Discov.* 6:827–837. <https://doi.org/10.1158/2159-8290.CD-15-1545>

Chou, R., J.L. Gore, D. Buckley, R. Fu, K. Gustafson, J.C. Griffin, S. Grusing, and S. Selph. 2015. Urinary Biomarkers for Diagnosis of Bladder Cancer: A Systematic Review and Meta-analysis. *Ann. Intern. Med.* 163:922–931. <https://doi.org/10.7326/M15-0997>

Choueiri, T.K., M.N. Fishman, B. Escudier, D.F. McDermott, C.G. Drake, H. Kluger, W.M. Stadler, J.L. Perez-Gracia, D.G. McNeel, B. Curti, et al. 2016. Immunomodulatory Activity of Nivolumab in Metastatic Renal Cell Carcinoma. *Clin. Cancer Res.* 22:5461–5471. <https://doi.org/10.1158/1078-0432.CCR-15-2839>

Daud, A.I., K. Loo, M.L. Pauli, R. Sanchez-Rodriguez, P.M. Sandoval, K. Taravati, K. Tsai, A. Nosrati, L. Nardo, M.D. Alvarado, et al. 2016. Tumor immune profiling predicts response to anti-PD-1 therapy in human melanoma. *J. Clin. Invest.* 126:3447–3452. <https://doi.org/10.1172/JCI87324>

de Boer, E.C., W.H. de Jong, A.P.M. van der Meijden, P.A. Steerenberg, F. Witjes, P.D.J. Vegt, F.M.J. Debruyne, and E.J. Ruitenberg. 1991a. Leukocytes in the urine after intravesical BCG treatment for superficial bladder cancer. A flow cytometric analysis. *Urol. Res.* 19:45–50. <https://doi.org/10.1007/BF00294021>

De Boer, E.C., W.H. De Jong, A.P.M. Van Der Meijden, P.A. Steerenberg, J.A. Witjes, P.D.J. Vegt, F.M.J. Debruyne, and E.J. Ruitenberg. 1991b. Presence of activated lymphocytes in the urine of patients with superficial bladder cancer after intravesical immunotherapy with bacillus Calmette-Guérin. *Cancer Immunol. Immunother.* 33:411–416. <https://doi.org/10.1007/BF01741603>

Gooden, M.J., G.H. de Bock, N. Leffers, T. Daemen, and H.W. Nijman. 2011. The prognostic influence of tumour-infiltrating lymphocytes in cancer: a systematic review with meta-analysis. *Br. J. Cancer.* 105:93–103. <https://doi.org/10.1038/bjc.2011.189>

Gros, A., P.F. Robbins, X. Yao, Y.F. Li, S. Turcotte, E. Tran, J.R. Wunderlich, A. Mixon, S. Farid, M.E. Dudley, et al. 2014. PD-1 identifies the patient-specific CD8<sup>+</sup> tumor-reactive repertoire infiltrating human tumors. *J. Clin. Invest.* 124:2246–2259. <https://doi.org/10.1172/JCI73639>

Grossman, H.B., R.B. Natale, C.M. Tangen, V.O. Speights, N.J. Vogelzang, D.L. Trump, R.W. de Vere White, M.F. Sarosdy, D.P. Wood Jr., D. Raghavan, and E.D. Crawford. 2003. Neoadjuvant chemotherapy plus cystectomy compared with cystectomy alone for locally advanced bladder cancer. *N. Engl. J. Med.* 349:859–866. <https://doi.org/10.1056/NEJMoa022148>

Herbst, R.S., J.-C. Soria, M. Kowanzet, G.D. Fine, O. Hamid, M.S. Gordon, J.A. Sosman, D.F. McDermott, J.D. Powderly, S.N. Gettinger, et al. 2014. Predictive correlates of response to the anti-PD-L1 antibody MPDL3280A in cancer patients. *Nature.* 515:563–567. <https://doi.org/10.1038/nature14011>

Inozume, T., K. Hanada, Q.J. Wang, M. Ahmadzadeh, J.R. Wunderlich, S.A. Rosenberg, and J.C. Yang. 2010. Selection of CD8<sup>+</sup>PD-1<sup>+</sup> lymphocytes in fresh human melanomas enriches for tumor-reactive T cells. *J. Immunother.* 33:956–964. <https://doi.org/10.1097/CJI.0b013e3181fad2b0>

Kansy, B.A., F. Concha-Benavente, R.M. Srivastava, H.B. Jie, G. Shayan, Y. Lei, J. Moskovitz, J. Moy, J. Li, S. Brandau, et al. 2017. PD-1 Status in CD8<sup>+</sup> T Cells Associates with Survival and Anti-PD-1 Therapeutic Outcomes in Head and Neck Cancer. *Cancer Res.* 77:6353–6364. <https://doi.org/10.1158/0008-5472.CAN-16-3167>

Liakou, C.I., A. Kamat, D.N. Tang, H. Chen, J. Sun, P. Troncoco, C. Logothetis, and P. Sharma. 2008. CTLA-4 blockade increases IFN $\gamma$ -producing CD4<sup>+</sup>ICOS<sup>hi</sup> cells to shift the ratio of effector to regulatory T cells in cancer patients. *Proc. Natl. Acad. Sci. USA.* 105:14987–14992. <https://doi.org/10.1073/pnas.0806075105>

Mariathasan, S., S.J. Turley, D. Nickles, A. Castiglioni, K. Yuen, Y. Wang, E.E. Kadel III, H. Koepfen, J.L. Astarita, R. Cubas, et al. 2018. TGF $\beta$  attenuates tumour response to PD-L1 blockade by contributing to exclusion of T cells. *Nature.* 554:544–548. <https://doi.org/10.1038/nature25501>

McGranahan, N., A.J. Furness, R. Rosenthal, S. Ramskov, R. Lyngaa, S.K. Saini, M. Jamal-Hanjani, G.A. Wilson, N.J. Birkbak, C.T. Hiley, et al. 2016. Clonal neoantigens elicit T cell immunoreactivity and sensitivity to immune checkpoint blockade. *Science.* 351:1463–1469. <https://doi.org/10.1126/science.aaf1490>

Murugan, A., T. Mora, A.M. Walczak, and C.G. Callan Jr. 2012. Statistical inference of the generation probability of T-cell receptors from sequence repertoires. *Proc. Natl. Acad. Sci. USA.* 109:16161–16166. <https://doi.org/10.1073/pnas.1212755109>

Oakes, T., J.M. Heather, K. Best, R. Byng-Maddick, C. Husovsky, M. Ismail, K. Joshi, G. Maxwell, M. Noursadeghi, N. Riddell, et al. 2017. Quantitative Characterization of the T Cell Receptor Repertoire of Naïve and Memory Subsets Using an Integrated Experimental and Computational Pipeline Which Is Robust, Economical, and Versatile. *Front. Immunol.* 8:1267. <https://doi.org/10.3389/fimmu.2017.01267>

Pal, S.K., Y.I. Lin, B. Yuh, K. DeWalt, A. Kazarian, N. Vogelzang, and R.A. Nelson. 2015. Conditional Survival in de novo Metastatic Urothelial Carcinoma. *PLoS One.* 10:e0136622. <https://doi.org/10.1371/journal.pone.0136622>

Paley, M.A., D.C. Kroy, P.M. Odorizzi, J.B. Johnnidis, D.V. Dolfi, B.E. Barnett, E.K. Bikoff, E.J. Robertson, G.M. Lauer, S.L. Reiner, and E.J. Wherry. 2012. Progenitor and terminal subsets of CD8<sup>+</sup> T cells cooperate to contain chronic viral infection. *Science.* 338:1220–1225. <https://doi.org/10.1126/science.1229620>



- Patel, M.R., J. Ellerton, J.R. Infante, M. Agrawal, M. Gordon, R. Aljumaily, C.D. Britten, L. Dirix, K.-W. Lee, M. Taylor, et al. 2018. Avelumab in metastatic urothelial carcinoma after platinum failure (JAVELIN Solid Tumor): pooled results from two expansion cohorts of an open-label, phase 1 trial. *Lancet Oncol.* 19:51–64. [https://doi.org/10.1016/S1470-2045\(17\)30900-2](https://doi.org/10.1016/S1470-2045(17)30900-2)
- Pieraerts, C., V. Martin, P. Jichlinski, D. Nardelli-Haeffliger, and L. Derre. 2012. Detection of functional antigen-specific T cells from urine of non-muscle invasive bladder cancer patients. *Oncol Immunology.* 1:694–698. <https://doi.org/10.4161/onci.20526>
- Powles, T., P.H. O'Donnell, C. Massard, H.T. Arkenau, T.W. Friedlander, C.J. Hoimes, J.L. Lee, M. Ong, S.S. Sridhar, N.J. Vogelzang, et al. 2017. Efficacy and Safety of Durvalumab in Locally Advanced or Metastatic Urothelial Carcinoma: Updated Results From a Phase 1/2 Open-label Study. *JAMA Oncol.* 3:e172411. <https://doi.org/10.1001/jamaoncol.2017.2411>
- Powles, T., I. Durán, M.S. van der Heijden, Y. Loriot, N.J. Vogelzang, U. De Giorgi, S. Oudard, M.M. Retz, D. Castellano, A. Bamias, et al. 2018. Atezolizumab versus chemotherapy in patients with platinum-treated locally advanced or metastatic urothelial carcinoma (IMvigor211): a multicentre, open-label, phase 3 randomised controlled trial. *Lancet.* 391:748–757. [https://doi.org/10.1016/S0140-6736\(17\)33297-X](https://doi.org/10.1016/S0140-6736(17)33297-X)
- Reading, J.L., F. Gálvez-Cancino, C. Swanton, A. Lladser, K.S. Peggs, and S.A. Quezada. 2018. The function and dysfunction of memory CD8<sup>+</sup> T cells in tumor immunity. *Immunol. Rev.* 283:194–212. <https://doi.org/10.1111/imr.12657>
- Rizvi, N.A., M.D. Hellmann, A. Snyder, P. Kvistborg, V. Makarov, J.J. Havel, W. Lee, J. Yuan, P. Wong, T.S. Ho, et al. 2015. Cancer immunology. Mutational landscape determines sensitivity to PD-1 blockade in non-small cell lung cancer. *Science.* 348:124–128. <https://doi.org/10.1126/science.1257621>
- Roederer, M., J.L. Nozzi, and M.C. Nason. 2011. SPICE: exploration and analysis of post-cytometric complex multivariate datasets. *Cytometry A.* 79:167–174. <https://doi.org/10.1002/cyto.a.21015>
- Sakuishi, K., L. Apetoh, J.M. Sullivan, B.R. Blazar, V.K. Kuchroo, and A.C. Anderson. 2010. Targeting Tim-3 and PD-1 pathways to reverse T cell exhaustion and restore anti-tumor immunity. *J. Exp. Med.* 207:2187–2194. <https://doi.org/10.1084/jem.20100643>
- Sharma, P., Y. Shen, S. Wen, S. Yamada, A.A. Jungbluth, S. Gnjatich, D.F. Bajorin, V.E. Reuter, H. Herr, L.J. Old, and E. Sato. 2007. CD8 tumor-infiltrating lymphocytes are predictive of survival in muscle-invasive urothelial carcinoma. *Proc. Natl. Acad. Sci. USA.* 104:3967–3972. <https://doi.org/10.1073/pnas.0611618104>
- Sharma, P., M. Retz, A. Siefker-Radtke, A. Baron, A. Necchi, J. Bedke, E.R. Plimack, D. Vaena, M.O. Grimm, S. Bracarda, et al. 2017. Nivolumab in metastatic urothelial carcinoma after platinum therapy (CheckMate 275): a multicentre, single-arm, phase 2 trial. *Lancet Oncol.* 18:312–322. [https://doi.org/10.1016/S1470-2045\(17\)30065-7](https://doi.org/10.1016/S1470-2045(17)30065-7)
- Snyder, A., V. Makarov, T. Merghoub, J. Yuan, J.M. Zaretsky, A. Desrichard, L.A. Walsh, M.A. Postow, P. Wong, T.S. Ho, et al. 2014. Genetic basis for clinical response to CTLA-4 blockade in melanoma. *N. Engl. J. Med.* 371:2189–2199. <https://doi.org/10.1056/NEJMoa1406498>
- Thommen, D.S., J. Schreiner, P. Müller, P. Herzig, A. Roller, A. Belousov, P. Umansky, P. Posa, C. Klein, M. Bacac, et al. 2015. Progression of Lung Cancer Is Associated with Increased Dysfunction of T Cells Defined by Coexpression of Multiple Inhibitory Receptors. *Cancer Immunol. Res.* 3:1344–1355. <https://doi.org/10.1158/2326-6066.CCR-15-0097>
- Thommen, D.S., V.H. Koelzer, P. Herzig, A. Roller, M. Trefny, S. Dimeloe, A. Kiialainen, J. Hanhart, C. Schill, C. Hess, et al. 2018. A transcriptionally and functionally distinct PD-1<sup>+</sup> CD8<sup>+</sup> T cell pool with predictive potential in non-small-cell lung cancer treated with PD-1 blockade. *Nat. Med.* 24:994–1004. <https://doi.org/10.1038/s41591-018-0057-z>
- Togneri, F.S., D.G. Ward, J.M. Foster, A.J. Devall, P. Wojtowicz, S. Alyas, F.R. Vasques, A. Oumie, N.D. James, K.K. Cheng, et al. 2016. Genomic complexity of urothelial bladder cancer revealed in urinary cfDNA. *Eur. J. Hum. Genet.* 24:1167–1174. <https://doi.org/10.1038/ejhg.2015.281>
- Tumeh, P.C., C.L. Harview, J.H. Yearley, I.P. Shintaku, E.J. Taylor, L. Robert, B. Chmielowski, M. Spasic, G. Henry, V. Ciobanu, et al. 2014. PD-1 blockade induces responses by inhibiting adaptive immune resistance. *Nature.* 515:568–571. <https://doi.org/10.1038/nature13954>
- Van Allen, E.M., D. Miao, B. Schilling, S.A. Shukla, C. Blank, L. Zimmer, A. Sucker, U. Hillen, M.H.G. Foppen, S.M. Goldinger, et al. 2015. Genomic correlates of response to CTLA-4 blockade in metastatic melanoma. *Science.* 350:207–211. <https://doi.org/10.1126/science.1260095>
- Zappasodi, R., S. Budhu, M.D. Hellmann, M.A. Postow, Y. Senbabaoglu, S. Manne, B. Gasmi, C. Liu, H. Zhong, Y. Li, et al. 2018. Non-conventional Inhibitory CD4. *Cancer Cell.* 33:1017–1032.e7. <https://doi.org/10.1016/j.ccell.2018.05.009>